Hamedan University of Technology
Iranian Association of Electrical and Electronics Engineers

Sustainable Energy and Artificial Intelligence

Online ISSN: 3060-8015

Journal Homepage: www.enai.hut.ac.ir

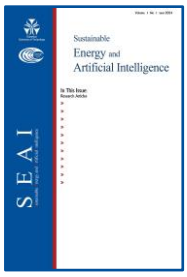

Integrated Optimization of Solar-Based Multi-Generation Systems for Cooling, Heating, Power, and Freshwater with Different Prime Movers

Amin Saleh*, Vahid Ghamar, Hassan Hajabdollahi

Department of Mechanical Engineering, Faculty of Engineering, Vali-e-Asr University, Rafsanjan, Iran
** Corresponding Author: Amin.Saleh@stu.vru.ac.ir*

Article Info

Article type:
Original Article

Article history:
Received 2025-08-01;
Revised 2025-09-01;
Accepted 2025-10-01.

How to cite this article:
Saleh, A., Hajabdollahi, H. and Ghamari, V., (2025). Integrated Optimization of Solar-Based Multi-Generation Systems for Cooling, Heating, Power, and Freshwater with Different Prime Movers. *Sustainable Energy and Artificial Intelligence*, *1*(2), 1-14.
DOI: 10.61882/seai.2508-1032

Abstract

The proposed solar-assisted hybrid system integrates decentralized, energy-efficient technologies for multi-vector energy production, delivering key advantages such as improved efficiency, lower emissions, economic feasibility, sustainability, and enhanced reliability. This work investigates the optimal design of a solar–fossil-fuel-based configuration capable of generating cooling, heating, power, and freshwater (CCHPW). The system employs different prime movers for combined heat and power production, namely a gas engine (GE), gas turbine (GT), and solid oxide fuel cell (SOFC). The overall plant consists of a prime mover, two types of chillers, an auxiliary boiler, a reverse osmosis desalination unit, parabolic trough solar collectors, a proton exchange membrane (PEM) electrolyzer, and thermal and cooling energy storage systems. A genetic algorithm is utilized to minimize the total annual cost (TAC). Optimization results demonstrate that the exergy efficiency of the GE-based CCHPW system is about 40.31% and 92.50% higher than that of SOFC- and GT-based systems, respectively. Moreover, the GE configuration achieves reductions in TAC of 27.08% and 23.80% compared to SOFC and GT systems, respectively.

***Keywords*:** Thermo-Economic Optimization, Solar Energy, Energy Storage Tank, Prime Mover, Genetic Algorithm.

1. Introduction

The escalating challenges posed by growing energy use and environmental concerns have prioritized energy saving, consumption minimization, sustainable resource management, and efficiency improvement for policymakers and communities alike [1,2]. Combined cooling, heating, and power (CCHP) systems are a promising solution for producing multiple forms of energy simultaneously [3,4]. Nevertheless, selecting an appropriate prime mover is critical, especially as many CCHP systems rely on fossil fuels. Solid oxide fuel cells (SOFCs) are environmentally friendly options, emitting minimal pollutants like SOx and NOx [5,6]. Desalination, particularly of seawater, is a vital solution for regions with rapid population growth and freshwater scarcities. Incorporating desalination into cogeneration systems has proven to reduce energy demands significantly [7,8]. Solar energy, a key renewable resource, offers pollution-free power but requires high initial investment [9]. Solar-based cogeneration systems combined with energy storage tanks can further enhance efficiency by minimizing cooling and thermal energy waste from prime movers and chillers. This integrated approach offers a sustainable path to meeting

energy and water needs [10]. Previous studies have analyzed multigenerational systems from various perspectives.

Xu et al. [11] conducted a comprehensive study to determine the optimum capacity of the prime mover in a CCHP system. Their research incorporated thermodynamic, environmental and economic factors to identify the most efficient system design. The optimized CCHP system exhibited an impressive exergy efficiency of 55.53% and an energy efficiency of 68.79%. Additionally, a combined approach of solar energy and cogeneration systems has been proposed as an efficient solution to address both energy and environmental challenges. Yang et al. [12] studied a CCHP system incorporating solar thermal collectors and photovoltaic (PV) panels with various tracking approach. Their research indicated that the fixed temperature load (FTL) technique is generally the preferred method for system operation. Hou et al. [13] explored a solar-based CCHP system, focusing on its design, operational strategies, and facility capacities. The system integrated multiple advanced technologies, including SOFC, solar evacuated tube collectors (ETC), PV panels, electrical and absorption chillers, and thermal energy storage (TES) tanks. Their optimization of the CCHP system demonstrated significant energy efficiency, achieving an annual increase in heat output of 170183 MJ and saving approximately 15141.63 kWh of electricity compared to standalone systems.

Saleh et al. [14] focused on optimizing a solar-powered combined cooling, heating, power, freshwater, and hydrogen (CCHPWH) generation system. It utilized parabolic trough collectors (PTC), TES and cooling energy storage (CES) tanks, proton exchange membrane (PEM) electrolyzers, and multi-effect evaporation with thermal vapor compression (MEE-TVC), including constant partial load (CPL) and variable partial load (VPL) for chillers. Various configurations were compared. The findings showed that the CCHPWH + TES + PTC + CES system with VPL strategy achieved a lower total annual cost (TAC) compared to the CPL strategy. Chitgar et al. [15] investigated an innovative cogeneration system integrating a SOFC with reverse osmosis (RO) desalination to simultaneously produce electricity and freshwater, assessing from energy, exergy, and economic perspectives. The system delivers about 1.3 MW of power and 226 m^3 of freshwater per day, achieving an exergy efficiency of 54% with a total operating cost of 36.80 $/h. Forghani et al. [16] optimized a multi-generation system for cooling, heating, power, and freshwater production. Their innovative approach incorporated TES and CES tanks. The outcomes revealed that integrating energy storage reduced the TAC by 11.30%.

A review of prior studies highlights advancements in multi-generation systems integrating thermal and electrical desalination, particularly with solar energy. Efficient thermal management and energy storage improve performance and reduce emissions, while hydrogen production from waste energy offers potential benefits. Selecting an optimal prime mover (PM) is key to balancing energy supply and demand across diverse configurations. A comprehensive investigation is needed, covering PM selection, energy storage, solar integration, and desalination. This study aims to optimize the design and operation of multi-generation systems with different PMs to efficiently meet varied demands. To accomplish this goal, the objectives of the current study are outlined as below:

- This research optimizes a solar-fossil fuel-powered system producing cooling, heating, power, and freshwater (CCHPW) for a hot climate, using thermal and cooling storage tanks, and generating oxygen and hydrogen as byproducts.
- The 12-month design, based on monthly averages, includes prime mover (SOFC, gas engine (GE) and gas turbine (GT)), auxiliary boiler, TES and CES tanks, PTCs, electrical and absorption chillers, PEM electrolyzer and RO unit as components.
- A genetic algorithm (GA) minimizes total annual cost (TAC), and the optimal results from different prime movers are compared.

2. System Explanation

Fig. 1 illustrates a solar-assisted fuel combined cooling, heating, power, and freshwater generation system that includes cooling and thermal energy storage tanks. At the core of this multi-generation system is a prime mover capable of simultaneously producing power and heat. The work examines different prime movers, such as SOFC, GE, and GT, with a RO unit used for desalination. The heat recovered from the prime mover meets the heating demand, while an auxiliary boiler supplements any heat shortfall. Cooling demands are addressed by both absorption and electrical chillers, and the RO unit fulfills freshwater requirements. Cooling and thermal energy storage tanks are integrated to store excess heating and cooling loads from each month for use in the next months. Solar parabolic trough

collectors (PTCs) are employed to meet heating demand loads. Additionally, the system allows for the sale or purchase of electricity from the grid. The PEM electrolyzer utilizes the recovered power from brine water pressure to generate oxygen and hydrogen as byproducts.

3. Thermal Modeling

The presumptions underlying the thermal modeling of the proposed configuration are as below:

- Heat losses are neglected in the analysis.
- Electricity exchange with the grid (both purchase and sale) is allowed.
- Ninety-five percent of the heat produced by the prime mover is recovered via a heat exchanger.
- The efficiency of electricity transmission through the grid is considered to be 92%.
- Freshwater is assumed to be salt-free.
- The auxiliary boiler and one of the chillers can be off, with their capacities set to zero.

Ambient temperature, demand load, and solar radiation are averaged on a monthly basis. Consequently, the total electricity demand load is estimated as below [14]:

$$\dot{E}_{dmn,tot} = \dot{E}_{dmn} + PL_{ch,\,el} \times \frac{\dot{Q}_{ch,el,\,nom}}{COP_{ch,el,\,PL}} + \dot{E}_{dmn,RO} \quad (1)$$

here, $\dot{E}_{dmn}$, $PL_{ch,\,el}$, $COP_{ch,\,el,\,PL}$, $\dot{Q}_{ch,\,el,\,nom}$, and $\dot{E}_{dmn,\,RO}$ refer to electricity demand load, partial load (PL), coefficient of performance at PL, nominal capacity of the electrical chiller, and the electricity consumption of the RO unit. The nominal capacity of the electrical chiller is determined as below [14]:

$$\dot{Q}_{ch,el,\,nom} = \alpha \times \dot{Q}_{dmn,\,max} \quad (2)$$

where, α represents the electric cooling ratio, which denotes the fraction of the total cooling demand that is supplied by the electric chiller. It is mathematically expressed as [14]:

$$\alpha = \frac{\dot{Q}_{ch,el}}{\dot{Q}_{dmn}} \quad (3)$$

This study utilizes PM, an auxiliary boiler, and PTCs to supply the heating demand load. The overall heating demand load, comprising both absorption chiller energy consumption and direct heating loads, is estimated as follows [14]:

$$\dot{H}_{dmn,tot} = \dot{H}_{dmn} + PL_{ch,\,ab} \times \frac{\dot{Q}_{ch,ab,\,nom}}{COP_{ch,ab,\,PL}} + \dot{H}_{HX,\,PEM} \quad (4)$$

where, $\dot{H}_{dmn}$, $\dot{Q}_{ch,\,ab,\,nom}$, $COP_{ch,\,ab,\,PL}$, $PL_{ch,\,ab}$, and $\dot{H}_{HX,\,PEM}$ imply heating demand load, nominal capacity, PL, and coefficient of performance at PL of absorption chiller, and PEM electrolyzer heating utilization, respectively. Nominal capacity of absorption chiller is expressed as follows [14]:

$$\dot{Q}_{ch,ab,\,nom} = (1-\alpha) \times \dot{Q}_{dmn,\,max} \quad (5)$$

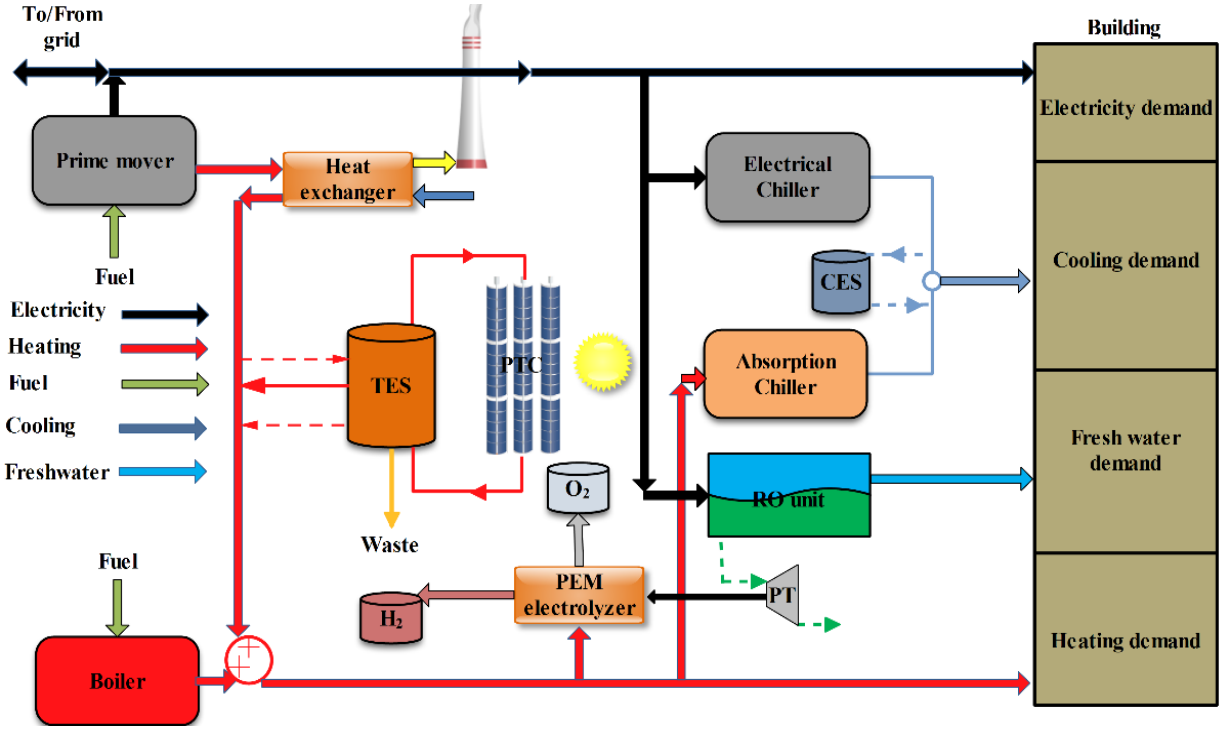

Fig. 1. Schematic diagram of a solar-fossil fuel multi-generation system with energy storage tanks.

The electrical power generation and the amount of heat recovered from the system's prime movers under PL conditions can be expressed as follows [13,17]:

- ***SOFC***

$$\dot{E}_{SOFC} = \dot{m}_{f,\,SOFC} \times \eta^{PL}_{SOFC,\,e} \quad (6)$$

$$\dot{H}_{SOFC} = \dot{m}_{f,\,SOFC} \times \eta^{PL}_{SOFC,\,h} \quad (7)$$

$$\eta^{PL}_{SOFC,\,e} = A_1 PL^3_{SOFC} + B_1 PL^2_{SOFC} + C_1 PL_{SOFC} + D_1 \quad \& \quad PL_{SOFC} = \frac{\dot{E}_{SOFC}}{\dot{E}_{nom,\,SOFC}} \quad (8)$$

$$\eta^{PL}_{SOFC,\,h} = A_2 PL^3_{SOFC} + B_2 PL^2_{SOFC} + C_2 PL_{SOFC} + D_2 \quad (9)$$

where, $\dot{E}_{SOFC}$, $\dot{m}_{SOFC}$, $\eta^{PL}_{SOFC,\,e}$ and $\eta^{PL}_{SOFC,\,h}$ refer to generated electrical power, the mass flow rate of fuel consumption, and the efficiencies of both electricity production and heat recovery for the SOFC at partial load are determined as follows. The parameters A, B, C, and D represent constant values obtained from Ref [13].

- ***GE***

$$\frac{\dot{E}_{GE,\,PL}}{\dot{m}_{f,PL} LHV_f} = (-0.0001591 \times (PL)^2 + 0.024 \times (PL) + 0.1904) \times \eta_{GE,nom} \quad (10)$$

$$\frac{\dot{H}_{oil,GE,\,PL}}{\dot{m}_{f,PL} LHV_f} = 2.157 \times 10^{-8} \times (PL)^4 - 9.866 \times 10^{-6} \times (PL)^3 + 0.001897 \times (PL)^2 - 0.1897 \times (PL) + 12.71 \quad (11)$$

$$\frac{\dot{H}_{wj,GE,\,PL}}{\dot{m}_{f,PL} LHV_f} = 17.49 \times exp(-0.07512 \times (PL)) + 39.36 \times exp(-0.002556 \times (PL)) \quad (12)$$

$$\frac{\dot{H}_{exh,GE,\,PL}}{\dot{m}_{f,PL} LHV_f} = 8.56 \times exp(-0.02619 \times (PL)) + 18.91 \times exp(0.001194 \times (PL)) \quad (13)$$

$$\frac{\dot{m}_{f,PL}}{\dot{m}_{f,nom}} = 0.2408 \times exp\left(0.01403 \times (PL)\right) + 0.3553 \times exp\left(-0.02494 \times (PL)\right) \quad (14)$$

$$\dot{m}_{f,nom} = \frac{\dot{E}_{nom}}{\eta_{nom} LHV_f} \quad (15)$$

where, $\dot{E}_{GE,\,PL}$, $\dot{H}_{wj,\,GE,\,PL}$, $\dot{H}_{oil,\,GE,\,PL}$ and $\dot{H}_{exh,\,GE,\,PL}$ represent generation of electricity, water jacket, lubricating oil and exhaust gas heat recovered from GE, respectively. LHV_f is lower heating value of fuel (natural gas) and $\dot{m}_{f,\,PL}$ refer to mass flow rate of fuel at PL of GE. Plus, $\dot{m}_{f,\,nom}$ is nominal fuel mass flow rate, and η_{nom} is nominal efficiency of GE and is evaluated as below [14,17]:

$$\eta_{GE,nom} = (0.00097 \times E_{nom} + 37.5)/100 \quad (16)$$

$$\frac{\eta_{GE,PL}}{\eta_{GE,nom}} = (-0.0001591 \times (PL)^2 + 0.024 \times (PL) + 0.1904) \quad (17)$$

here, E_{nom} is nominal capacity of GE.

- ***GT***

$$\frac{\dot{E}_{GT,PL}}{\dot{m}_{f,PL} LHV_f} = \frac{-0.002551 (PL)^2 + 1.135 (PL) + 11.71}{100} \times \eta_{GT,nom} \quad (18)$$

$$\frac{\dot{H}_{exh,GT,PL}}{\dot{m}_{f,PL} LHV_f} = 0.0061 \times (PL) + 0.3868 \quad (19)$$

$$\frac{\dot{m}_{f,PL}}{\dot{m}_{f,nom}} = 0.4772 \times exp\left(0.007565 \times (PL)\right) - 0.2123 \times exp\left(-0.02677 \times (PL)\right) \quad (20)$$

here, $\dot{E}_{GT,\,PL}$ and $\dot{H}_{exh,\,GT,\,PL}$ are generation of electricity and exhaust gas heat recovered of GT, respectively. $\dot{m}_{f,\,PL}$ is mass flow rate of fuel at PL of GT. Nominal efficiency of GT is estimated as below [14,17]:

$$\eta_{GT,nom} = 1.22 \times \left(\frac{-9.2 \times 10^{-8} \times E^2_{nom} + 0.001724 \times}{E_{nom} + 18.1}\right)/100 \quad (21)$$

Thus, GT efficiency at PL is estimated as:

$$\frac{\eta_{GT,PL}}{\eta_{GT,nom}} = -0.002551 \times (PL)^2 + 1.135 (PL) + 11.71 \quad (22)$$

- ***Chillers***

$$\frac{COP_{ch,el,PL}}{COP_{el,nom}} = 1.819 (PL) - 0.819 (PL)^2 \quad (23)$$

$$\frac{COP_{ch,ab,PL}}{COP_{ab,nom}} = \frac{PL}{0.75 (PL)^2 + 0.0195 (PL) + 0.213} \quad (24)$$

$$\dot{E}_{ch,el} = \frac{\dot{Q}}{COP_{ch,el}} \quad (25)$$

$$\dot{H}_{ch,ab} = \frac{\dot{Q}}{COP_{ch,ab}} \quad (26)$$

where, $COP_{ab,\,nom}$ and $COP_{el,\,nom}$ are nominal coefficient of performance of absorption and electrical chillers and are equal 3 and 0.7, respectively [14,17]. Additionally, $\dot{H}_{ch,\,ab}$ and $\dot{E}_{ch,\,el}$ are the essential heat and electricity of absorption and electrical chiller.

- ***Auxiliary Boiler***

The auxiliary boiler provides the necessary heating capacity to meet any shortfall or the total heating demand load. The efficiency at PL and fuel mass flow rate of the auxiliary boiler are given as below [14]:

$$\frac{\eta_{b,PL}}{\eta_{b,nom}} = 0.0951 + 1.525 (PL) - 0.6249 (PL)^2 \quad (27)$$

$$\dot{m}_{f,b} = \frac{\dot{H}_b}{\eta_b LHV_f} \quad (28)$$

- ***Solar Parabolic Trough (PTC) Collector***

The collectors utilized were of the Euro Trough 100 (ET100) model. Hourly solar irradiation was estimated using the equations provided in Ref [18]. The total heat generated by the ET100 collectors and their efficiency are calculated as follows [19]:

$$\dot{Q}_{Useful}=Gb\times\eta_{ET100}\times n_{mirror}\times A_{mirror}/1000 \quad (29)$$

$$\eta_{ET100}=0.75-0.000045\times(T_{in}-T_{out})-0.039\times\left(\frac{T_{in}-T_{out}}{Gb}\right)-0.003\times Gb\times\left(\frac{T_{in}-T_{out}}{Gb}\right)^{2} \quad (30)$$

here, Gb, A_{mirror}, η_{ET100} and n_{mirror} are solar irradiation, each mirror area, collector efficiency and the number of mirrors, respectively. To ensure effective system control under varying conditions during the year, Therminol VP-1 (TVP1) is selected as the heat transfer fluid due to its high boiling point. Its specific heat capacity can be determined using the provided equation [19]:

$$Cp_{TVP1}=+0.002414\times T+5.9591\times T^{-6}\times T^{2}-2.9879\times 10^{-8}\times T^{3}+4.4172\times 10^{-11}\times T^{4}+1.498 \quad (31)$$

- ***RO Unit***

Reverse Osmosis has been one of the most significant desalination methods in recent decades. With recent advancements, RO unit has developed into a leading technology, demonstrating exceptional performance in meeting the growing global demand for freshwater. This research uses the mathematical model of the RO plant developed by Dessouky [20]. The thermodynamic modeling and the governing energy relations for the RO unit are detailed in reference [20].

- ***PEM Electrolyzer***

The operation of the PEM electrolyzer involves heating water to its operating temperature via a heat exchanger. The water is then separated into its constituent elements, oxygen and hydrogen. The oxygen-water mixture is separated, with unreacted water returned to the cycle for further hydrogen production. The resulting oxygen and hydrogen are stored. Detailed information on the PEM electrolyzer modeling can be found in Ref [14].

- ***TES and CES Tanks***

The heating demand is primarily met by recovered heat from the prime mover, but due to seasonal variations, surplus heat is stored in a TES tank. The TES operates in charge and discharge modes, with an auxiliary boiler supplying heat when needed. Similarly, a CES tank balances cooling demand fluctuations by storing excess chiller output and supplying cooling when needed. The TES and CES tank models are detailed in Ref [14].

4. Exergy Analysis

Exergy is a measure of the quality of energy, considering the specific environmental conditions. It represents the maximum amount of work that can be produced from a given energy source. The exergy efficiency of a CCHPW system is calculated by comparing the useful work output to the total work input as [14]:

$$\eta_{ex}=\frac{\sum_{t=1}^{n}\left[\dot{E}_{dmn}+\left(1-\frac{T_o}{T_{Heat}}\right)\dot{H}_{dmn}-\left(1-\frac{T_o}{T_{cool}}\right)\dot{Q}_{dmn}+\dot{E}x_{f_w}+\dot{E}x_{H_2}\right]\times\tau_t}{\sum_{t=1}^{n}\left[\dot{E}x_{f,\,input}+\dot{E}_{buy}+\dot{E}x_{f,PTC}\right]\times\tau_t} \quad (32)$$

where, T_o, $T_{cool}=278.15$ (k) and $T_{Heat}=363.15$ (k) are ambient temperature, cooling demand temperature and heating demand temperature, respectively.

5. Optimization Method and Objective Function

Owing to the inherent complexity of the cogeneration system, characterized by nonlinear interdependencies among variables, restrictive operational constraints, and the necessity for optimization, the genetic algorithm (GA) has been adopted as the optimization methodology. In contrast to Mixed-Integer Nonlinear Programming (MINLP) approaches, GA is capable of effectively managing continuously varying decision variables that cannot be reduced to binary representations. Furthermore, the use of GA circumvents the limitations of MINLP techniques by eliminating the need for oversimplifying assumptions, thereby enabling a more comprehensive and accurate representation of the optimization problem [17]. The genetic algorithm is used to optimize the system and minimize its TAC. The optimization process involves 5000 generations, with a population size of 400 individuals. The genetic operators, crossover and mutation, are applied with probabilities of 0.8 and 0.025, respectively. The objective function selected is the TAC, and stated as below:

$$TAC(\$/year)=\sum_{i=1}^{n}(a\times\beta\times C_{inv})_i+\sum_{j=1}^{k}\left[\dot{E}_{buy,j}\times\theta_{e,buy}+\dot{m}_{f,j}\times\theta_{f,j}\times LHV_f-\dot{E}_{sell,j}\times\theta_{e,sell}+C_{em,j}\right]\times\tau_j \quad (33)$$

The capacity of the PM, its PL at 12 units, mass flow rate of PTCs, electric cooling ratio (α), PL at 16 units for chillers (8 for each chiller), auxiliary boiler capacity, TES tank capacity, CES tank capacity, operating temperature of PEM and high-pressure pump isentropic efficiency in RO unit are considered as the 36 decision variables to select the minimum TAC. Design parameters are presented in Table 1.

Table 1. Design parameters, their range and step of variation.

Parameters	From	To	Step
PM capacity (kW)	0	6000	100
PL of SOFC (%)	25	100	5
PL of GT, GE (%)	20	100	5
Auxiliary boiler capacity (kW)	0	6000	100
Absorption chiller PL (%)	0	100	10
Electrical chiller PL (%)	0	100	10
TES tank capacity (kW)	0	8000	100
CES tank capacity (kW)	0	8000	100
Electric cooling ratio (%)	0	1	0.01
Mass flow rate of PTC (kg/s)	0	10	1
HP pump efficiency (%)	70	80	1
PEM operating temperature (°C)	40	80	1

Additionally, Fig 2. indicates modeling and optimization flowchart. The flowchart illustrates the step-by-step procedure adopted for the optimization process using a GA. Initially, design variables and system parameters are defined, and a population matrix is generated. Each chromosome is decoded to form a parameter set, from which the thermal and power output of the prime mover and the solar contribution from parabolic trough collectors are calculated. Subsequently, the performance of absorption and electrical chillers, the desalination unit, and the PEM electrolyzer are determined. Energy and heating balances are evaluated, followed by charge–discharge calculations of the thermal and cooling energy storage units. For each time step, the TAC is computed. The algorithm then checks the number of chromosomes and applies GA operators including selection, crossover, mutation, and elitism. This iterative process continues until the predefined maximum number of generations (5000) is reached, ensuring convergence to the optimal multi-generation system configuration. The components investment cost and some economic parameters are presented in Refs [13, 14, 21]. Total annual cost reduction percent (TACR) of CCHPW system in comparison with different prime movers is evaluated as below:

$$TACR = \frac{TAC_{CCHPW}^{Max} - TAC_{CCHPW}^{Min}}{TAC_{CCHPW}^{Max}} \times 100 \quad (34)$$

The percent of operational cost (OC) reduction (OCR) of CCHPW system in comparison with different prime movers is estimated as follows:

$$OCR = \frac{OC_{CCHPW}^{Max} - OC_{CCHPW}^{Min}}{OC_{CCHPW}^{Max}} \times 100 \quad (35)$$

6. Environmental Assessment

Enhancing system performance contributes to lowering pollutant emissions. While recent research has extensively explored energy and exergy analysis, relatively limited attention has been devoted to environmental aspects. To address this gap, the present study incorporates an environmental assessment that accounts for CO_2 emissions from fuel combustion and evaluates the associated penalties for pollutant release, outlined as [15]:

$$C_{em} = \sum_{j=1}^{k} \left[3600 \times \dot{m}_{CO2,j} \times \omega_{em,\,CO2}\right]$$
$$\dot{m}_{CO2} = \sum_{j=1}^{k} \dot{m}_{f,j} \times LHV_f \times \mu_{em,\,CO2} \quad (36)$$

7. Results and Discussion

This study investigates a solar-fossil fuel multi-generation system. The system utilizes various prime movers (GE, GT, and SOFC) to generate electricity and heat. To improve system efficiency and reduce emissions, TES and CES tanks, PTCs are incorporated. Additionally, the system includes a RO unit for freshwater production and an auxiliary boiler for supplemental heating shortfall. The multi-generation system is implemented for a region located in the southwest of Iran (Bushehr province along the Persian Gulf), characterized by a hot climate and acceptable solar radiation. To simplify the system, the demands, solar irradiation and ambient temperature are averaged for each month. Solar irradiation and ambient temperature are shown in Fig. 3. Moreover, Fig. 3 shows the cooling, heating, power and freshwater demand in a hot climate.

Validation of the results was conducted by comparing the performance of each proposed component with findings from authoritative scientific sources; the outcomes of this comparative assessment are presented below.

Fig. 4a illustrates the performance of the SOFC under different PL conditions. The SOFC simultaneously produces electricity and heat. At a PL of 25%, the system achieves its highest efficiency in heat generation. Conversely, when operating between 70% and 95% PL, the SOFC exhibits superior efficiency in electricity production. At maximum load, the efficiencies of heat and electricity generation become approximately equal.

Fig. 4b demonstrates that as the PL of the gas turbine increases, its power output correspondingly rises. However, the recoverable exhaust energy remains nearly unchanged, since the exhaust outlet temperature stays approximately constant.

Fig. 4c illustrates the energy distribution in the gas engine, where the input fuel is converted into power along with recovered heat from the exhaust gases, lubricating oil, and cooling water jacket. At lower PL conditions, the engine operates at reduced rotational speed, leading to higher heat recovery from the cooling water jacket and lower recovery from the lubricating oil. As PL increases, the engine speed rises, resulting in a decrease in jacket water heat recovery and an increase in lubricating oil heat recovery. The power output continues to improve with rising PL up to about 80%. Beyond this point, frictional losses become dominant, causing a decline in output power. Therefore, the GE achieves its optimum thermal performance at approximately 80% PL.

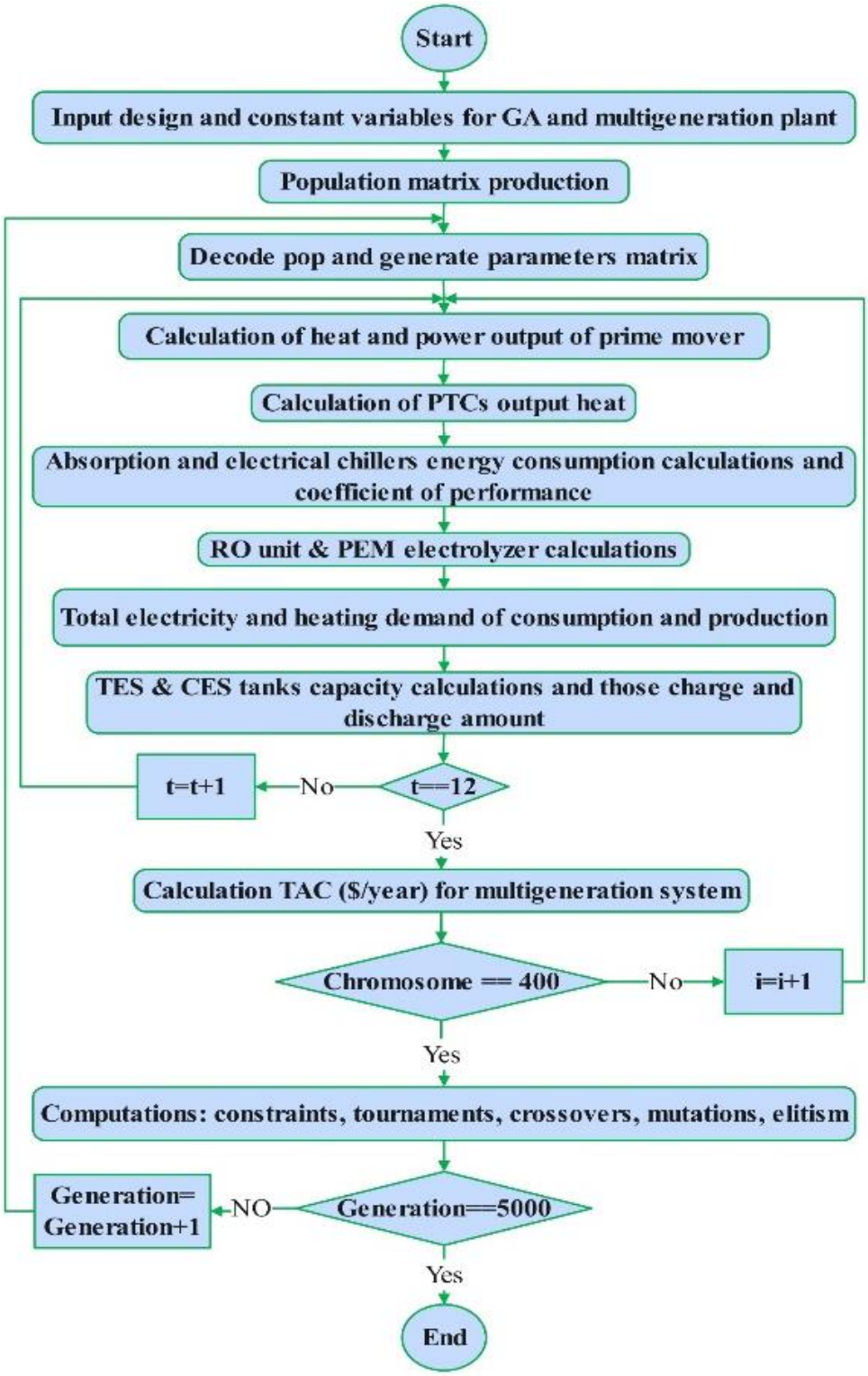

Fig. 2. Flowchart of modeling and optimization.

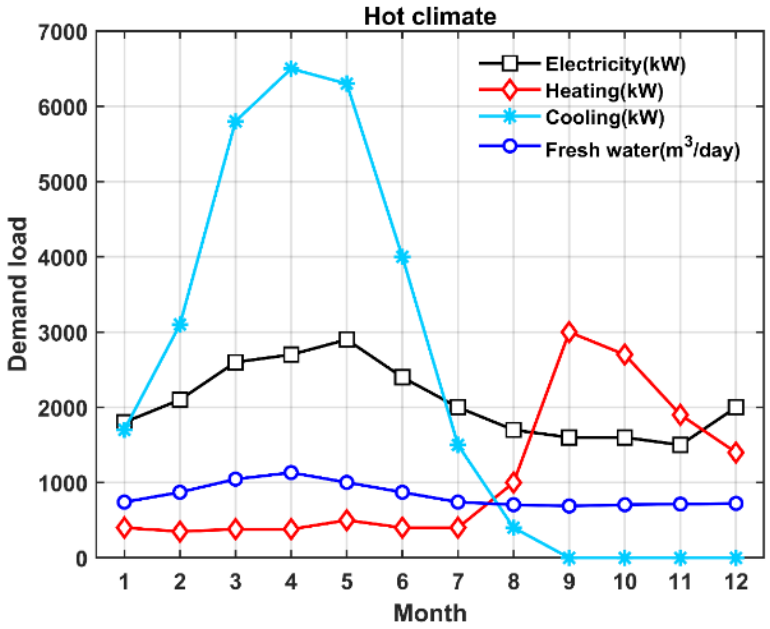

Fig. 3. Monthly average cooling, heating, power, and freshwater demands load during the year.

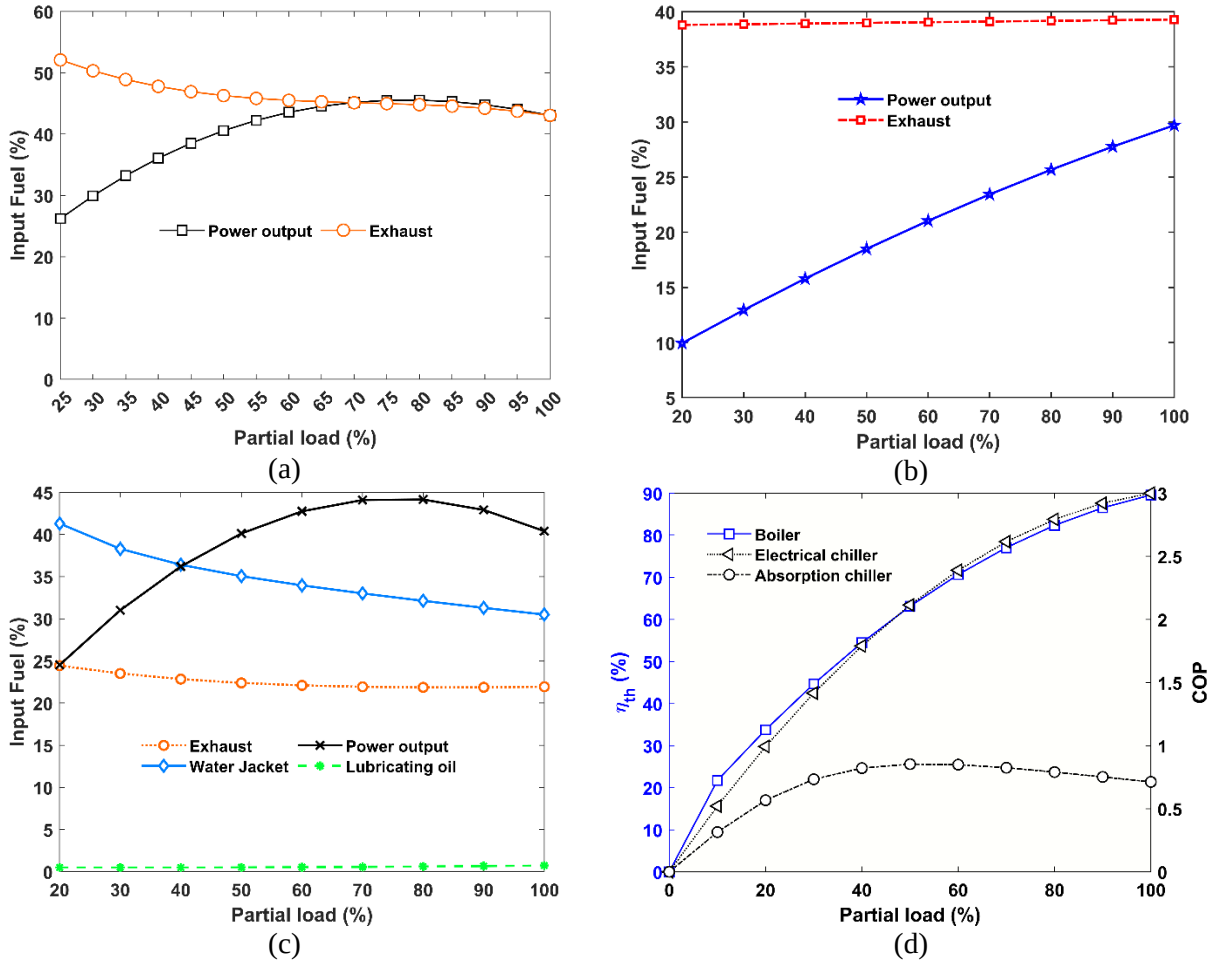

Fig. 4. Energy performance of a) SOFC, b) GT, c) GE, and (d) the boiler and chillers.

In this study, the chillers are considered under PL operation, as variations in PL directly influence their performance. As shown in Fig. 4d, the coefficient of performance (COP) of the electrical chiller improves with increasing PL, while the absorption chiller exhibits its optimal performance at approximately 50% PL. Moreover, the thermal efficiency of the boiler is enhanced as PL increases.

To validate the RO unit, its operating parameters were compared with those reported in Ref [22]. As presented in Table 2, the results obtained from the current RO model show good agreement with the reference system, with the maximum deviation being less than 5.5%, which is considered acceptable and within allowable limits.

Fig. 5 presents a comparison between the results of the current PEM electrolyzer model and the data reported in Ref [23] for current density (J_{PEM}) and cell potential (V). The results indicate that as the current density increases, the cell voltage initially rises sharply, after which the growth rate slows and continues with a more gradual upward trend.

Table 2. Comparison of the current RO unit with Ref [22].

Parameter	Current model	Ref	Diff (%)
m_d (m^3/h)	145.8	-----	----
m_f (m^3/h)	485.9	485.9	0.00
m_b (m^3/h)	340.2	340.1	0.00
X_b (ppm)	64177	64180	0.00
X_d (ppm)	250.2	250	0.00
SR	0.9944	0.9944	0.00
ΔP (kPa)	6843.1	6850	0.10
SPC (kWh/m^3)	7.81	7.68	1.69
$\dot{W}_P$, (kW)	1190	1131	5.27

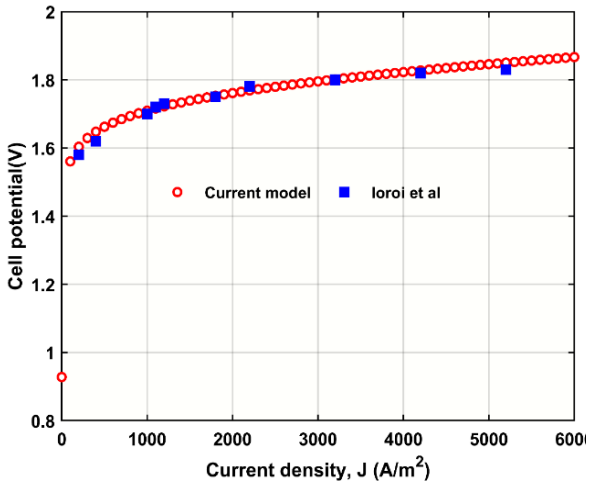

Fig. 5. the PEM electrolyzer model results with the Ioroi et al [23].

The optimal results of multi-generation system with various prime movers are listed in Table 3. The capacity of GE is higher compared to those of SOFC and GT. Notably, the auxiliary boiler capacity in the CCHPW system with GE is zero. Due to these and selling and buying electricity cost, showing the scenario with GE is more effective from the perspective of simultaneous electricity and heating compared to SOFC and GT. The PTCs has proven effective in CCHPW systems with GT and SOFC. It is evident that solar thermal collectors are suitable for integration in these cases. In the CCHPW system with all PMs, both TES and CES tanks are considered, as the incorporation of energy storage tanks enhances the economic and thermodynamic performance of the multi-generation system. In terms of investment cost, the CCHPW system incorporating GE and GT show a lower total investment cost compared to CCHPW system with SOFC. It is mainly due to higher investment costs of new technologies such as SOFC compared to conventional PMs. The exergy efficiency of the CCHPW system with GE is approximately 40.31% and 92.50% higher than that of the SOFC and GT systems, respectively. Plus, the optimum total annual cost and exergy efficiency were determined to be 1.6708×10^6 $/year and 42.08 %, respectively, for the system utilizing the gas engine. According to the maximum capacity of the RO unit, the freshwater production, power consumption, specific power consumption of it, and Pelton turbine (PT) power production were at 14.3 kg/s, 298.75 kW, 5.81 kWh/m^3 and 95.5 kW, respectively. Moreover, the power production of the PT is utilized by the PEM electrolyzer to produce H2 and O2. The PEM electrolyzer achieves a mass flow rate of 9912.3 kg/year and 78671 kg/year for H_2 and O_2 production.

In this configuration, the PT power output is directed to the PEM electrolyzer for hydrogen and oxygen production. Figure 15.b presents the mass flow rates of H2 and O2, with maximum daily production values of 37.65 kg/day and 298.78 kg/day, respectively. The overall exergetic efficiency of the PEM electrolyzer is determined to be 58.89%.

Fig. 5 illustrates the exergy efficiency of the CCHPW system with different prime movers. The results highlight that the system's performance is strongly influenced by the partial load of the prime mover. When the gas engine (GE) is employed, the CCHPW system consistently demonstrates higher exergy efficiency compared with the solid oxide fuel cell (SOFC) and gas turbine (GT). Moreover, the variation in efficiency for systems with SOFC and GT is narrower than that observed with GE, since SOFC and GT typically operate at full load throughout the year, whereas GE operates under varying partial loads. The GE-based system also follows a more uniform efficiency trend across the year. In the early months, when GE operates more frequently at full load, the system efficiency is relatively lower, whereas in the later months, efficiency improves. In contrast, the SOFC- and

GT-based systems display the opposite seasonal trend. The maximum exergy efficiencies achieved are approximately 33.58% for SOFC, 26.49% for GT, and 49.27% for GE.

Table 3. Optimal results of system performance and design parameters.

Design parameters	GE	SOFC	GT
PM nominal capacity (kW)	4600	2100	2200
Electrical chiller capacity (kW)	3250	1885	0
Absorption chiller capacity (kW)	3250	4615	6500
Auxiliary boiler capacity (kW)	0	1100	3300
Electric cooling ratio (%)	50	29	0
CES capacity (kW)	2700	4200	3500
TES capacity (kW)	300	1000	2000
Mass flow rate of PTC (kg/s)	0	5.4	4.5
HP pump efficiency (%)	80	80	80
System performance			
Total investment cost ($) $\times 10^6$	6.5472	9.4917	6.5653
Fuel cost ($/year) $\times 10^5$	6.4926	4.0046	7.7097
Environmental cost ($/year) $\times 10^5$	3.2525	1.9905	3.8037
Buying electricity cost from the grid ($/year) $\times 10^5$	0	3.5044	1.5284
Selling electricity Cost to the grid ($/year) $\times 10^5$	2.3286	0.057365	0.43077
Exergy efficiency (%)	42.08	29.99	21.86
TAC ($/year) $\times 10^6$	1.6708	2.2912	2.1928

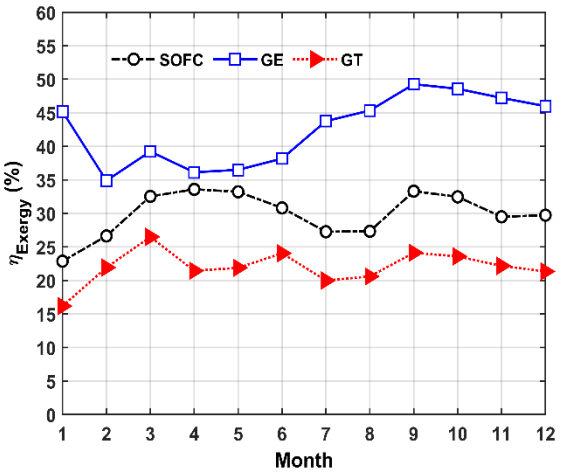

Fig. 5. Exergy efficiency of system with different PMs.

Fig. 6 presents the operating costs (OC) associated with the combined cooling, heating, power and freshwater (CCHPW) system across different prime movers (PMs). The data indicate that fuel costs represent a substantial proportion of the OC in all cases. Furthermore, the carbon dioxide emissions (CDE) account for the second-largest share of operating costs in all cases, except for the configuration utilizing the SOFC as the PM. Notably, the CCHPW system employing a GE demonstrates the lowest OC, whereas the configuration incorporating a GT incurs the highest OC. When GE is utilized as the PM, the OCR is evaluated by 41.19% and 21.49% relative to the GT and SOFC configurations, respectively.

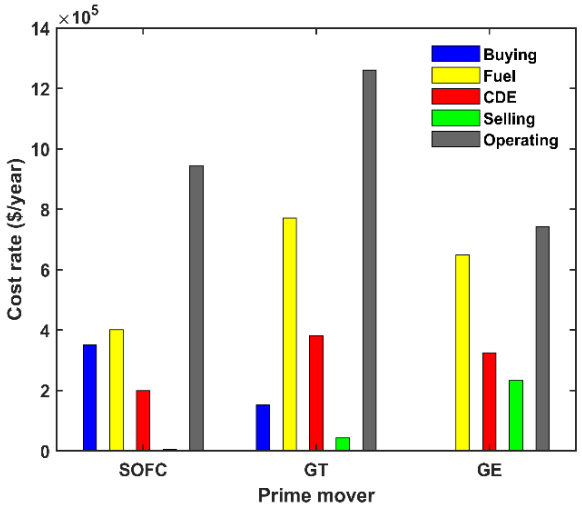

Fig. 6. The operating costs of proposed system.

This section concludes by presenting the TAC results. According to Table 2 and equation 32, the optimal CCHPW system with GE achieves a 27.08% and 23.80% reduction in TAC compared to systems with SOFC and GT, respectively.

Fig. 7 shows the optimal PL operation of the equipment within the CCHPW system. In all configurations, the PL of the RO unit decreases in response to reduced freshwater demand. For systems incorporating a gas turbine and solid oxide fuel cell, an auxiliary boiler is included and operated up to 100% PL, as higher boiler loading enhances thermal efficiency. The gas engine is operated within a PL range of 60–90% throughout the year, whereas the GT and boiler are typically utilized at full load. The SOFC exhibits variable loading, ranging from 80–100%, primarily due to improved thermal efficiency within these intervals. The electrical chiller demonstrates increasing coefficient of performance with rising PL, leading to operation above 40% PL. Similarly, the absorption chiller operates within a

40–100% PL range owing to its higher COP under these conditions.

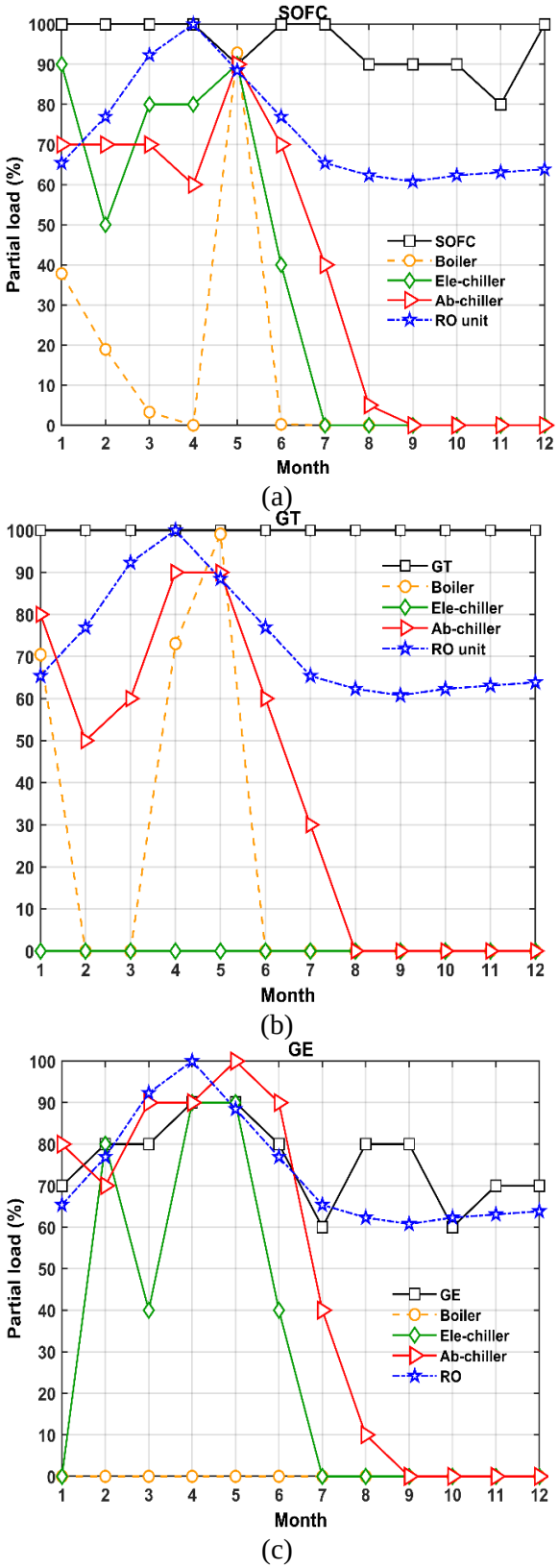

Fig. 7. The optimal partial load of component in proposed configuration with, a) SOFC, b) GT and c) GE

Fig. 8 presents the distribution of investment costs among the main components of the CCHPW system for different prime movers: SOFC, GT, and GE. The results clearly indicate that the prime mover and the reverse osmosis unit constitute the largest shares of capital cost in all system configurations. In the SOFC-based system, the PM accounts for about 45.22% of the total investment, followed by the RO unit at 28.46%, while other components such as chillers, TES/CES tanks, boiler, and PEM electrolyzer collectively represent less than 30%. Similarly, for the GT configuration, the RO unit (41.14%) and the PM (20.12%) dominate the investment, with chillers (17.39%) and ET100 (14.24%) also contributing significantly. In the GE-based system, the PM (41.13%) and the RO unit (41.26%) almost equally share the highest portion of costs, while chillers (15.18%) rank third, and the remaining components contribute marginally.

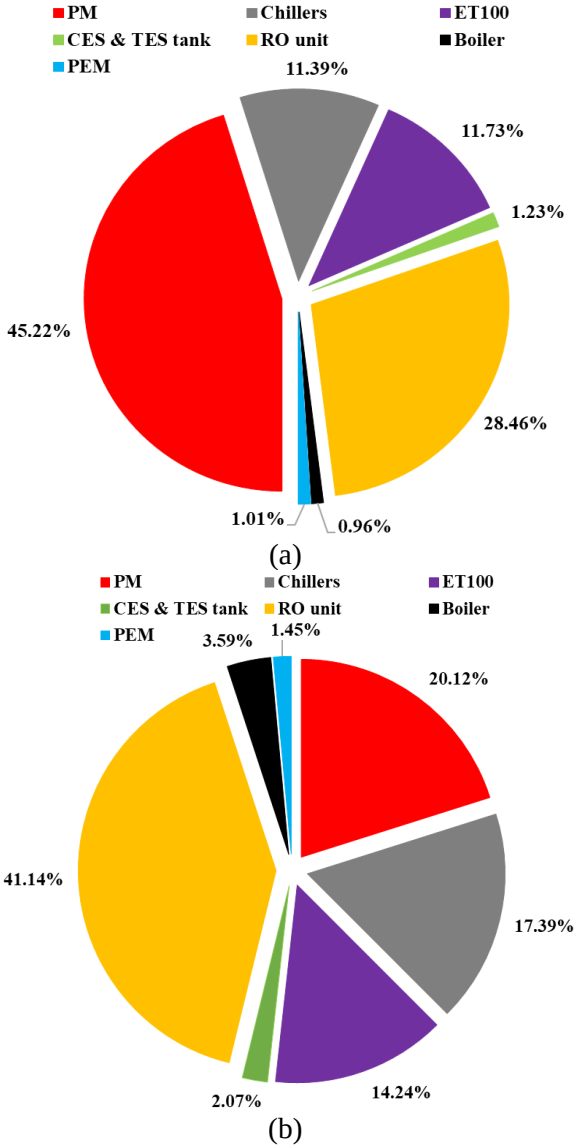

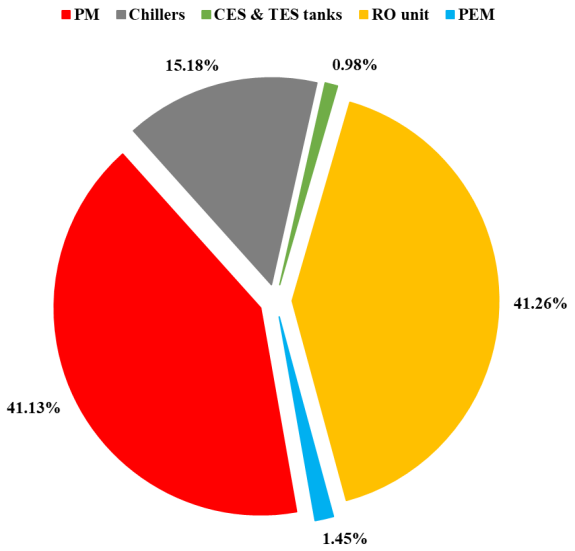

(c)

Fig. 8. The investment cost of component in proposed configuration with, a) SOFC, b) GT and c) GE.

These findings emphasize that the prime mover selection and the desalination subsystem are the most cost-intensive elements of the multi-generation plant. The auxiliary boiler, TES/CES storage units, and PEM electrolyzer consistently incur the lowest investment costs across all cases.

Fig 9 indicates the sensitivity analysis of the total annual cost with respect to the partial load of the CCHPW system. The results highlight that operating strategy and PL conditions of major components substantially influence the system's economic performance, further underlining the importance of optimal load management and prime mover configuration.

8. Conclusion

This study focused on the design and optimization of a hybrid solar-fossil fuel multi-generation system for producing cooling, heating, electricity, and freshwater, with hydrogen and oxygen as byproducts. The optimization method considered genetic algorithm and total annual cost as the objective function. The system's prime movers included gas engine, gas turbines, and solid oxide fuel cell. The optimal results highlighted the effectiveness of PTCs in systems with GT and SOFC. Both TES and CES tanks were integrated in all configurations. Based on economic outcomes, the prime mover selection and the desalination subsystem are the most cost-intensive elements of the multi-generation plant. The optimal system, featuring GE, achieved a total annual cost of 1.6708×10^{6} \$/year and an exergy efficiency of 42.08%.

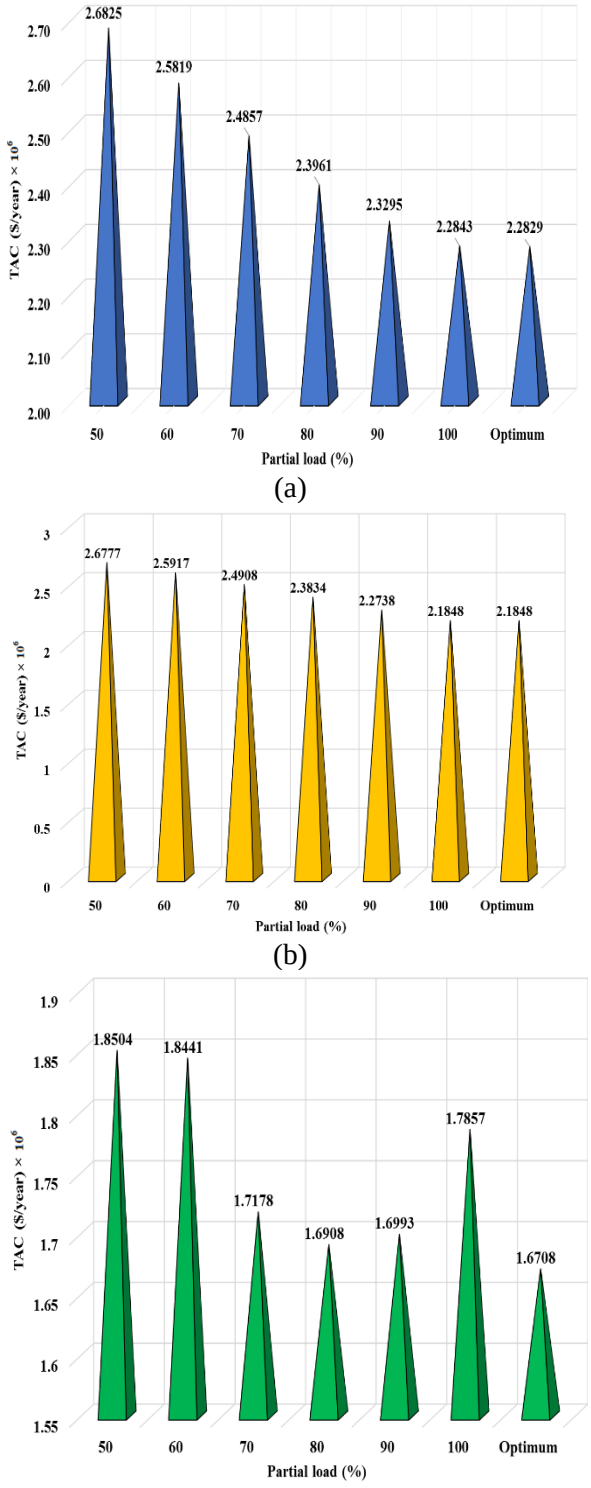

(a)

(b)

(c)

Fig. 9. The sensitivity analysis of TAC at PL in proposed configuration with, a) SOFC, b) GT and c) GE.

References

[1] Wang, J., & Azam, W. (2024). Natural resource scarcity, fossil fuel energy consumption, and total greenhouse gas emissions in top emitting countries. *Geoscience frontiers*, *15*(2), 101757.

[2] Saleh, A., Ghamari, V., & Hajabdollahi, H. (2025).

Efficient design of solar-fossil fuel multi-generation system using artificial intelligence. *Applied Thermal Engineering*, 127231.
[3] Zhang, Y. (2025). Optimization of combined cooling, heating, and power systems with thermal energy storage using a modified genetic algorithm. *Journal of Building Engineering*, 112780.
[4] Salimi, M., Hosseinpour, M., Mansouri, S., & N. Borhani, T. (2022). Environmental aspects of the combined cooling, heating, and power (CCHP) systems: a review. *Processes*, *10*(4), 711.
[5] Ma, W., Han, W., Liu, Q., & Xu, G. (2023). A Review of Combined Heat and Power (CHP).
[6] Ling, X., Liang, Y., Zhao, M., Shen, J., Zhu, Y., & Ye, K. (2025). Multi-criteria parameter analysis and optimization of a combined cooling, heating, and power system based on SOFC/GT and S-CO2/T-CO2 cycle. *Applied Thermal Engineering*, *272*, 126433.
[7] Sun, Q., Sun, Z., Hu, X., Zhang, W., & Wu, L. (2025). Optimizing integrated concentrated solar power and desalination systems with flexible design. *Energy Conversion and Management*, *326*, 119523.
[8] Khashehchi, M., Thangavel, S., Rahmanivahid, P., Heidari, M., Moazzeni, T., Verma, V., & Kumar, A. (2024). Solar desalination techniques: Challenges and opportunities. *Highly Efficient Thermal Renewable Energy Systems*, 305-329.
[9] Wang, G., Zhang, Z., & Lin, J. (2024). Multi-energy complementary power systems based on solar energy: A review. *Renewable and Sustainable Energy Reviews*, *199*, 114464.
[10] Rezaie, K., Mehrpooya, M., Delpisheh, M., & Noorpoor, A. (2024). Solar-driven chemisorption cogeneration system integrated with thermal energy storage. *Journal of Energy Storage*, *76*, 109705.
[11] Xu, J., Yao, Y., & Yousefi, N. (2021). Optimal prime mover size determination of a CCHP system based on 4E analysis. *Energy Reports*, *7*, 4376-4387.
[12] Yang, G., & Zhai, X. Q. (2019). Optimal design and performance analysis of solar hybrid CCHP system considering influence of building type and climate condition. *Energy*, *174*, 647-663.
[13] Hou, H., Wu, J., Ding, Z., Yang, B., & Hu, E. (2021). Performance analysis of a solar-assisted combined cooling, heating and power system with an improved operation strategy. *Energy*, *227*, 120516.
[14] Saleh, A., Hajabdollahi, H., Ghamari, V., & Dehaj, M. S. (2023). Evaluation of operational strategy of cooling and thermal energy storage tanks in optimal design of multi generation system. *Energy*, *284*, 129256.
[15] Chitgar, N., Emadi, M. A., Chitsaz, A., & Rosen, M. A. (2019). Investigation of a novel multigeneration system driven by a SOFC for electricity and fresh water production. *Energy conversion and management*, *196*, 296-310.
[16] Forghani, A. H., Hajabdollahi, H., & Solghar, A. A. (2024). Investigating the energy storage performance in optimal design of a solar hybrid multi-generation system with distillatory. *Energy Storage*, *6*(2), e609.
[17] Hajabdollahi, H., Saleh, A., Ghamari, V., & Dehaj, M. S. (2022). Technical and economic evaluation of the combined production cooling, heating, power, freshwater, and hydrogen (CCHPWH) system in the cold climate. *Journal of the Taiwan Institute of Chemical Engineers*, *133*, 104262.
[18] Sanaye, S., & Hajabdollahi, H. (2015). Thermo-economic optimization of solar CCHP using both genetic and particle swarm algorithms. *Journal of Solar Energy Engineering*, *137*(1).
[19] Hajabdollahi, H., Saleh, A., & Yadollahi, N. K. (2025). Multi-objective optimization of a solar-assisted cogeneration system in hot climate: An exergoeconomic and exergoenvironmental assessment. *Thermal Science and Engineering Progress*, 103656.
[20] El-Dessouky, H. T., & Ettouney, H. M. (2002). *Fundamentals of salt water desalination*. Elsevier.
[21] Hajabdollahi, H., Saleh, A., & Shafiey Dehaj, M. (2024). A multi-generation system based on geothermal driven: energy, exergy, economic and exergoenvironmental (4E) analysis for combined power, freshwater, hydrogen, oxygen, and heating production. *Environment, Development and Sustainability*, *26*(10), 26415-26447.
[22] Nafey, A. S., & Sharaf, M. A. (2010). Combined solar organic Rankine cycle with reverse osmosis desalination process: energy, exergy, and cost evaluations. *Renewable Energy*, *35*(11), 2571-2580.
[23] Ioroi, T., Yasuda, K., Siroma, Z., Fujiwara, N., & Miyazaki, Y. (2002). Thin film electrocatalyst layer for unitized regenerative polymer electrolyte fuel cells. *Journal of Power sources*, *112*(2), 583-587.

Biography

Amin Saleh is a PhD student at Vali-e-Asr University of Rafsanjan. His has published numerous articles in the field of thermal system design, hydrogen and fuel cell technologies, artificial intelligence applications in energy systems, and renewable energy. He is currently working at the combined cycle power plant of the South Pars Gas Complex, where he is involved in maintenance methods and planning.

Vahid Ghamari received his M.Sc. degree in Mechanical Engineering from Vali-e-Asr University of Rafsanjan, Rafsanjan, Iran, in 2020. He is currently a Ph.D. student in Mechanical Engineering at Vali-e-Asr University of Rafsanjan. His research interests include the design and optimization of energy systems, multi-effect and reverse osmosis desalination, energy storage, CHP, CCHP, and lithium-ion battery packs. He has published 12 research papers in Mechanical Engineering journals, and he has been a member of the National Elite Foundation of Iran since 2021.

Hassan Hajabdollahi is a Professor of Mechanical Engineering and faculty member of Vali Asr University of Rafsanjan. He has published numerous articles in the field of energy and optimization and is the author of the book Optimization of Heat Exchangers. His research interests include Multi Vector, Energy, Evolutionary Computation.